Calculation of Pulse Parameters and Propagation of Uncertainty

Paul D. Hale, *Senior Member, IEEE*, and C. M. Jack Wang

***Abstract*—The fundamental starting point for the analysis of all two-state waveforms is the determination of the low- and high-state levels. This is a two-step process. First, the data are grouped into points belonging to each state, and second, the value of each state is determined from the group mean, the mode, the median, or some other statistic. Once the state levels are determined, pulse parameters such as transition duration, amplitude, overshoot, and undershoot can be calculated. The IEEE 181-2003 Standard on Transitions, Pulses, and Related Waveforms recommends methods for grouping the data, determining the state levels, and determining pulse parameters, but gives no guidance for propagation of uncertainty, particularly in the presence of systematic and/or correlated sources of error. Correlations are important because certain pulse parameters, such as transition duration and pulse duration, are invariant with respect to, e.g., multiplicative error, which is correlated highly. We propose a new procedure for determining the pulse states that involves clustering the data and then using a robust location estimator to determine the state level. This technique allows the propagation of uncertainty from the covariance of a sampled waveform representation all the way to the calculation of pulse parameters. We use Monte Carlo simulations to verify the proposed procedure for some canonical pulse waveforms.**

***Index Terms*—Covariance analysis, metrology, oscilloscopes, pulse measurements, uncertainty.**

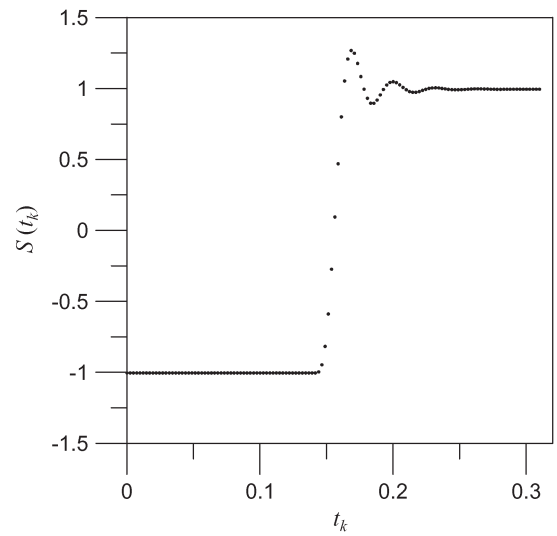

Fig. 1. Two-state waveform with nominal state levels $L_1 = -1.0000$ and $L_2 = 0.9897$. All operations in this paper are independent of any particular unit system; therefore, we consider them dimensionless. All quantities in this paper are scaled relative to either S or t as appropriate.

I. Introduction

OSCILLOSCOPES are routinely used to measure the properties of a wide variety of pulsed waveforms, including digital data streams in computers and in electrical and optical communications. Accurate characterization of pulse parameters and their measurement uncertainty has a huge economic impact on the producers and the consumers of the digital communications equipment and computers that are ubiquitous in modern everyday life. With cost pressures driving manufacturers to create products that just meet specifications, the ability to make robust and well-characterized measurements is becoming more important. In this paper, we describe a method that, given a mean waveform and its covariance, can be used to accurately calculate pulse parameters and their uncertainties, even in the presence of correlated errors. Correlations are important because certain pulse parameters, such as transition duration, are invariant with respect to, for example, multiplicative error, which is highly correlated in the example considered in this paper. The technique is totally general in that it can be extended to estimate the uncertainty of any scalar or vector quantity that is derived from the waveform.

Consider the two-state pulsed waveform in Fig. 1. The fundamental starting point for analysis of such a waveform is to group the samples in the waveform into groups that represent the low and high states of the waveform. The industry standard for pulse analysis is the IEEE 181-2003 Standard on Transitions, Pulses, and Related Waveforms [1]. In the absence of prior knowledge about the waveform, IEEE 181-2003 suggests making a histogram of the sampled waveform values. The histogram is then separated into lower and upper histograms from which the modes (or means) are computed and subsequently used to determine the waveform state levels. Once the state levels are estimated, pulse parameters such as amplitude, transition duration, overshoot, and undershoot can be calculated. IEEE 181-2003 describes how fluctuation in pulse parameters can be quantified; however, it gives no guidance on how to determine the total uncertainty of the determined pulse parameters.

Manuscript received September 10, 2007; revised May 1, 2008. First published September 30, 2008; current version published February 9, 2009. This work is a contribution of the National Institute of Standards and Technology and is not subject to copyright in the USA. The Associate Editor coordinating the review process for this paper was Dr. Jerome Blair.

P. D. Hale is with the Optoelectronics Division, National Institute of Standards and Technology, Boulder, CO 80305 USA (e-mail: hale@boulder.nist.gov).

C. M. J. Wang is with the Statistical Engineering Division, National Institute of Standards and Technology, Boulder, CO 80305 USA.

Digital Object Identifier 10.1109/TIM.2008.2005560

0018-9456/$25.00 © 2008 IEEE

Authorized licensed use limited to: IEEE Xplore. Downloaded on February 6, 2009 at 18:49 from IEEE Xplore. Restrictions apply.

Documentation of the pulse parameter measurement service that is previously implemented at the National Institute of Standards and Technology (NIST, USA) gives extensive details of how uncertainty analysis [2] of pulse parameter measurements could proceed. That analysis uses a propagation of uncertainty strategy that moves from physical phenomena directly to various pulse parameters. However, if a new (unforeseen) property of the waveform (along with its uncertainty) is required, it is necessary to start from the beginning. Unfortunately, the sensitivity of the new property to underlying physical phenomena may be unknown or uncharacterized. Even if the sensitivities are known, it is difficult to transport this information to the user in a convenient format. This paradigm makes it nearly impossible for the measurement service customer to estimate quantities (and associated uncertainties) other than those reported by the NIST.

The NIST measurement services are now being redesigned to make the whole waveform the quantity of interest. The goal of this paradigm shift is to provide the customer with the capability of calculating any required information from the calibrated waveform measurement. This is achieved by delivering the whole measured waveform along with the covariance matrix, which contains the uncertainty of each sampled point and the correlations between the errors in each sampled point. Although the NIST will still provide basic pulse parameter estimates that are extracted from the calibrated waveform, the customer will also be able to calculate other quantities (and their uncertainties) that might be of interest but are not provided by the NIST.

The analysis in [2] assumed that the physical phenomena underlying the pulse parameter errors are uncorrelated. This assumption is usually correct and is appropriate for the type of analysis that is described there. However, uncorrelated physical phenomena can lead to various correlations within a waveform that cannot be ignored in the "whole waveform" paradigm. For example, if correlations in pulse state levels due to multiplicative errors were ignored, the uncertainty in the pulse transition duration could be overestimated severely. "Tilt" [3] is another correlated error that can lead to variations in the pulse parameters. The covariance matrix allows the uncertainty, along with correlation information, to be transported from one customer (or procedure) to another in a convenient format. These uncertainties can include random and systematic effects.

The rest of this paper is organized as follows. Section II briefly reviews the covariance-based uncertainty analysis. In Section III, we present the procedures for determining state levels and their uncertainty covariance matrix. Section IV describes how the pulse parameters, such as transition duration, which are functions of the two state levels, are calculated. It also shows how the uncertainties of the pulse parameters are obtained by use of the covariance matrix approach. Section V describes in more detail some statistical considerations regarding additive and multiplicative errors. Section VI uses a simulation study to verify the covariance-based propagation of uncertainties for the pulse amplitude and the transition duration. We conclude with some summary remarks in Section VII.

II. Uncertainty Propagation

We use the covariance method described in [4] for the uncertainty propagation of multivariate quantities. Suppose that random vectors $\boldsymbol{X}$ $(m \times 1)$ and $\boldsymbol{Y}$ $(n \times 1)$ are related through a known functional relationship of the form

$$\boldsymbol{Y} = f(\boldsymbol{X}).$$

Then, the uncertainty of $\boldsymbol{Y}$ (expressed as a covariance matrix) can be estimated from the uncertainty of $\boldsymbol{X}$ as [5]

$$\boldsymbol{\Sigma}_Y = \mathrm{cov}(\boldsymbol{Y}) = \boldsymbol{J}\boldsymbol{\Sigma}_X\boldsymbol{J}^T \tag{1}$$

where $\boldsymbol{\Sigma}_X$ is the covariance matrix of $\boldsymbol{X}$, $\boldsymbol{J}^T$ denotes the transpose of $\boldsymbol{J}$, and $\boldsymbol{J}$ is an $n \times m$ Jacobian matrix with the (i, j)th element J_{ij} given by

$$J_{ij} = \frac{\partial Y_i}{\partial X_j}.$$

Equation (1) is exact if $f(\cdot)$ is linear in $\boldsymbol{X}$, i.e., if the matrix elements J_{ij} are independent of $\boldsymbol{X}$. It is approximate if $f(\cdot)$ is nonlinear. For example, suppose that

$$Y_1 = \frac{X_1}{X_2}\sin X_3$$
$$Y_2 = \frac{X_1}{X_2}\cos X_3.$$

Then

$$\boldsymbol{J} = \begin{pmatrix} \frac{\sin X_3}{X_2} & -\frac{X_1 \sin X_3}{X_2^2} & \frac{X_1 \cos X_3}{X_2} \\ \frac{\cos X_3}{X_2} & -\frac{X_1 \cos X_3}{X_2^2} & -\frac{X_1 \sin X_3}{X_2} \end{pmatrix}.$$

In a case that is relevant to this paper, consider a waveform vector $\boldsymbol{Y}$. Pulse parameters are functions of the two state levels, which, in turn, are functions of the waveform vectors. In this paper, we construct operators that transform the waveform vector into various pulse parameters and use (1) to derive the covariance matrix for the pulse parameters. This will be an effective method for determining the pulse parameter uncertainties if the covariance matrix of the waveform vector is available and if the algorithms and the associated operators are sufficiently linear. In Sections III and IV, we propose operators for determining state levels and reference times.

The International Standards Organization *Guide to the Expression of Uncertainty in Measurement* provides rules for evaluating and reporting the uncertainty only for the model of measurement having a single output quantity.[1] Several authors [6]–[9] have described methods for evaluating, expressing, and using the uncertainty that is associated with complex-valued quantities in radio frequency measurements. In this case, the input and output vectors are 2-D, and these methods are all

[1]An effort to produce a supplemental guide to the *Guide*, which includes measurement models with more than one output quantity, is being coordinated by the Joint Committee for Guides in Metrology. See http://www.bipm.org/en/committees/jc/jcgm/.

Authorized licensed use limited to: IEEE Xplore. Downloaded on February 6, 2009 at 18:49 from IEEE Xplore. Restrictions apply.

covariance based. A more general treatment of various multivariate measurement scenarios is given in [10]. A detailed description of how a covariance matrix representing a waveform measurement system might be constructed, including Type A and Type B evaluations of uncertainty, is given in [4]. A brief description of how some particular waveform covariance matrices can be obtained using Type A and Type B evaluations is given in Appendix A. A method for measuring a pulse that includes calibration at every time point inside the waveform epoch and a covariance matrix that can be used in the procedures described in this paper is reported in [11].

Finally, we note that uncertainties can be estimated using Monte Carlo simulation, such as the one described in [12]. This type of uncertainty analysis is more general than the covariance approach that we describe here because it can model the effects of system nonlinearities and different error probability distributions. These advantages come at the cost of considerable computer time for the simulations. We will use Monte Carlo simulations in Section VI to demonstrate that our operators are effectively linear, and that the covariance approach is valid for the applications that we describe here.

III. Determination of State Levels

As described in IEEE 181-2003, a *waveform epoch* that contains the waveform features under analysis is chosen. The waveform epoch must contain sufficient data to yield the state levels to the desired accuracy. Data points from the waveform must then be categorized or "clustered" as belonging to a particular state. We use the k-means method [13] to cluster the data. In this method, the samples are sorted by their distance from a particular cluster mean. Consider the pulse in Fig. 1 having two state levels with only one occurrence of each state. Let $\boldsymbol{Y} = (y_1, y_2, \ldots, y_I)$ be the waveform vector. The clustering process is iterative. We first select the initial cluster means; typically, we use (y_1, y_I) and assign y_i to the nearest cluster based on the distance between y_i and the cluster means. We then update the cluster means, which are calculated as the average values of y_i assigned to each cluster. The process continues until the y_i's no longer switch clusters or until the cluster means no longer change. After the algorithm converges, typically in two or three iterations, we obtain $Y_1 = \{y_1^{(1)}, y_2^{(1)}, \ldots, y_{I_1}^{(1)}\}$ as the set of all I_1 samples defining the state-one level (cluster one) and $Y_2 = \{y_1^{(2)}, y_2^{(2)}, \ldots, y_{I_2}^{(2)}\}$ the set of all I_2 samples defining the state-two level (cluster two).

Once the clusters are formed, we can use any of the location estimators, such as the arithmetic mean, the trimmed mean, the median, or the mode, to estimate the state levels [14]. Since waveform data may contain outliers, robust estimators should be used. The median and the least median of squares (LMS) estimator [15] can tolerate up to 50% of the outliers; that is, their breakdown points [16] are 50% (in contrast, the arithmetic mean has a breakdown point of 0; a single aberrant value can cause the mean to give an arbitrarily bad result). However, since there is not an adequate Jacobian matrix corresponding to the transformation of the waveform vectors to the median or the LMS estimator, it is difficult to employ the covariance approach for uncertainty propagation if either one of these estimators is used to estimate the state levels. Another choice is the mode [1], although uncertainty propagation is also difficult in this case.[2]

We use a location estimator, similar to the LMS estimator, of each cluster to estimate the state levels. For each cluster, the shortest interval that contains 50% of the data is determined. This approach is motivated by the need to find a "mode" without using the histogram method. The idea is that, instead of locating a (single-number) mode, we look for a concentration, or a "collective" mode, in the data. We use the "50% of the data" as the criterion for concentration. Instead of using the midpoint of the shortest interval, which is the LMS estimator of the data [15], we use the mean of the data contained in the shortest interval to estimate each state level. This allows us to easily obtain the approximate covariance matrix of the estimated state levels. The mean of the data in the shortest interval is sometimes called the "shorth" estimator.

For the set of I_1 samples that define the state-one level, the shortest interval that contains 50% of the I_1 samples is the interval that produces the smallest of the following differences:

$$y_{(h)}^{(1)} - y_{(1)}^{(1)},\ y_{(h+1)}^{(1)} - y_{(2)}^{(1)}, \ldots,\ y_{(I_1)}^{(1)} - y_{(I_1-h+1)}^{(1)}$$

where $h = \lfloor I_1/2 \rfloor + 1$, $\lfloor x \rfloor$ stands for the greatest integer less than or equal to x, and $y_{(1)}^{(1)} \leq y_{(2)}^{(1)} \leq \ldots \leq y_{(I_1)}^{(1)}$ are the ordered observations of $y_1^{(1)}, y_2^{(1)}, \ldots, y_{I_1}^{(1)}$. Let $(y_{(m)}^{(1)}, y_{(h+m-1)}^{(1)})$ be the shortest interval; then, the state level L_1 is calculated as

$$L_1 = \frac{1}{h} \sum_{j=m}^{h+m-1} y_{(j)}^{(1)}. \tag{2}$$

As a simple illustration, suppose that $I_1 = 11$ and

$$\left(y_{(1)}^{(1)}, \ldots, y_{(I_1)}^{(1)}\right) = (10, 45, 50, 53, 56, 58, 60, 62, 63, 65, 75).$$

Then, $h = \lfloor 11/2 \rfloor + 1 = 6$, and the smallest of the differences $58 - 10,\ 60 - 45,\ 62 - 50,\ 63 - 53,\ 65 - 56,$ and $75 - 58$ is 9, which corresponds to the interval (56, 65). The data contained in this interval are 56, 58, 60, 62, 63, and 65. The state level L_1 is calculated as $L_1 = (56 + 58 + 60 + 62 + 63 + 65)/6 = 60.67$.

Similarly, let $(y_{(n)}^{(2)}, y_{(k+n-1)}^{(2)})$ be the shortest interval that contains 50% of the I_2 samples defining the state level; then, the state level L_2 is calculated as

$$L_2 = \frac{1}{k} \sum_{j=n}^{k+n-1} y_{(j)}^{(2)} \tag{3}$$

where $k = \lfloor I_2/2 \rfloor + 1$.

The vector $\boldsymbol{L} = (L_1, L_2)^T$, representing the state levels, can be expressed as the linear transformation of $\boldsymbol{Y}$. That is,

$$\boldsymbol{L} = \boldsymbol{H}_L \boldsymbol{Y}$$

[2]The only method we know for estimating the uncertainty in the mode is through Monte Carlo simulation. It should be noted that the mode and its uncertainty are functions of the choice of the histogram bin size.

Authorized licensed use limited to: IEEE Xplore. Downloaded on February 6, 2009 at 18:49 from IEEE Xplore. Restrictions apply.

where $\boldsymbol{H}_L$ is a $2 \times I$ matrix. The ith element of the first row of $\boldsymbol{H}_L$ is

$$\begin{aligned} 1/h \quad & \text{if } y_j \in \left\{y_{(m)}^{(1)}, y_{(m+1)}^{(1)}, \ldots, y_{(h+m-1)}^{(1)}\right\} \\ 0 \quad & \text{if } y_j \notin \left\{y_{(m)}^{(1)}, y_{(m+1)}^{(1)}, \ldots, y_{(h+m-1)}^{(1)}\right\}. \end{aligned}$$

Similarly, the ith element of the second row of $\boldsymbol{H}_L$ is

$$\begin{aligned} 1/k \quad & \text{if } y_j \in \left\{y_{(n)}^{(2)}, y_{(n+1)}^{(2)}, \ldots, y_{(k+n-1)}^{(2)}\right\} \\ 0 \quad & \text{if } y_j \notin \left\{y_{(n)}^{(2)}, y_{(n+1)}^{(2)}, \ldots, y_{(k+n-1)}^{(2)}\right\}. \end{aligned}$$

Using (1), we estimate the covariance matrix $\boldsymbol{\Sigma}_L$ of $\boldsymbol{L}$ as

$$\boldsymbol{\Sigma}_L = \boldsymbol{H}_L \boldsymbol{\Sigma}_Y \boldsymbol{H}_L^T \tag{4}$$

where $\boldsymbol{\Sigma}_Y$ is the covariance matrix of $\boldsymbol{Y}$. The diagonal elements of $\boldsymbol{\Sigma}_L$ represent the variance of the two state levels of the pulse, whereas the off-diagonal elements represent the covariance of the state levels. However, (4) does not take into account the variation of the *process* of finding the shortest interval, which is nonlinear and nondifferentiable, and can underestimate the true variation of the state levels when uncorrelated errors are the main source of error. This point will be discussed further in Section V.

IV. Calculating Pulse Parameters and Propagation of Uncertainty

A. Pulse Amplitude

We define[3] the *pulse amplitude* A as

$$A = L_2 - L_1.$$

The squared standard uncertainty of the pulse amplitude is given by

$$u^2(A) = \boldsymbol{J}_{AL} \boldsymbol{\Sigma}_L \boldsymbol{J}_{AL}^T \tag{5}$$

where the Jacobian matrix $\boldsymbol{J}_{AL} = (-1, 1)$.

B. Reference Level Instant

According to [1], the $100 \times f$ percent *reference level* is defined as

$$y_r = L_1 + f(L_2 - L_1)$$

where $0 \leq f \leq 1$. Using our definition of L_1 and L_2, reference levels for $f < 0.5$ occur before those for $f > 0.5$. The *reference level instant* is the instant at which the waveform crosses the reference level and is generally estimated by interpolation of the waveform. The standard states that if the error due to linear interpolation "... is significant, then a more sophisticated interpolation method based on more than two adjacent samples may be used... The interpolation method and the conditions in which it is used must be specified." Here, we describe a method based on a polynomial fit of order P on a set of N samples closest to the percent reference level, where $P < N$, and P is typically one, two, or three.

We seek to find an estimate $\hat{t}_r$ of the reference level instant, i.e., the time at which the polynomial fit crosses the reference level y_r. For the following discussion, we assume that the time of the ith sample is t_i, and that the samples are sorted in order of increasing time. The N samples that are closest to the reference level are chosen. We then construct the vector $\boldsymbol{Y}_r = (y_{q+1}, \ldots, y_{q+N})^T$ of these N samples corresponding to times $(t_{q+1}, \ldots, t_{q+N})$. The vector $\boldsymbol{Y}_r$ can be expressed as the transformation

$$\boldsymbol{Y}_r = \boldsymbol{H}_r \boldsymbol{Y}$$

where $\boldsymbol{H}_r$ is an $N \times I$ matrix with only one nonzero element in each row, such that the ith element of the nth row of $\boldsymbol{H}_r$ is

$$\begin{aligned} 1 \quad & \text{if } i = q + n \\ 0 \quad & \text{if } i \neq q + n. \end{aligned}$$

That is, $\boldsymbol{H}_r$ is a transformation matrix that selects N elements of $\boldsymbol{Y}$ to form $\boldsymbol{Y}_r$.

We seek a weighted least-squares solution $\hat{\boldsymbol{\theta}}$ of the following equation:

$$\boldsymbol{M}\hat{\boldsymbol{\theta}} = \boldsymbol{Y}_r$$

where

$$\boldsymbol{M} = \begin{pmatrix} 1 & t_{q+1} & \cdots & t_{q+1}^P \\ \vdots & \vdots & \vdots & \vdots \\ 1 & t_{q+N} & \cdots & t_{q+N}^P \end{pmatrix}$$

and $\hat{\boldsymbol{\theta}} = (\hat{\theta}_0, \hat{\theta}_1, \ldots, \hat{\theta}_P)^T$ is the vector of estimated polynomial coefficients. The weighted least-squares estimate of the polynomial coefficients is [17]

$$\hat{\boldsymbol{\theta}} = \left(\boldsymbol{M}^T \boldsymbol{\Sigma}_r^{-1} \boldsymbol{M}\right)^{-1} \boldsymbol{M}^T \boldsymbol{\Sigma}_r^{-1} \boldsymbol{H}_r \boldsymbol{Y} \tag{6}$$

where

$$\boldsymbol{\Sigma}_r = \boldsymbol{H}_r \boldsymbol{\Sigma}_Y \boldsymbol{H}_r^T.$$

The estimated reference level instant is then the appropriate root of the following equation:

$$(\hat{\theta}_0 - y_r) + \hat{\theta}_1 \hat{t}_r + \cdots + \hat{\theta}_P \hat{t}_r^P = 0 \tag{7}$$

and the squared standard uncertainty corresponding to $\hat{t}_r$ is evaluated by propagation of uncertainty and is given by

$$u^2(\hat{t}_r) = \boldsymbol{J}_R \begin{pmatrix} \boldsymbol{\Sigma}_{\hat{\theta}} & \boldsymbol{\Sigma}_{\hat{\theta}L} \\ \boldsymbol{\Sigma}_{\hat{\theta}L}^T & \boldsymbol{\Sigma}_L \end{pmatrix} \boldsymbol{J}_R^T \tag{8}$$

where $\boldsymbol{J}_R$ is the Jacobian of the root of (7) with respect to $(\hat{\boldsymbol{\theta}}, \boldsymbol{L})$. Details of the root finding function and the Jacobian are worked out for a second-order polynomial fit in Appendix B.

[3] In this paper, we consider only pulses with a positive amplitude. However, the method we propose can be applied to both polarities.

Authorized licensed use limited to: IEEE Xplore. Downloaded on February 6, 2009 at 18:49 from IEEE Xplore. Restrictions apply.

The terms in the covariance matrix in (8) are found as follows. Making the substitution

$$\boldsymbol{T} = \left(\boldsymbol{M}^T \boldsymbol{\Sigma}_r^{-1} \boldsymbol{M}\right)^{-1} \boldsymbol{M}^T \boldsymbol{\Sigma}_r^{-1} \boldsymbol{H}_r$$

(6) can be rewritten as

$$\hat{\boldsymbol{\theta}} = \boldsymbol{T}\boldsymbol{Y}.$$

The covariance of $\hat{\boldsymbol{\theta}}$ is then given by

$$\boldsymbol{\Sigma}_{\hat{\theta}} = \boldsymbol{T}\boldsymbol{\Sigma}_Y \boldsymbol{T}^T = \left(\boldsymbol{M}^T \boldsymbol{\Sigma}_r^{-1} \boldsymbol{M}\right)^{-1}.$$

The polynomial coefficients may be correlated with the state levels of the waveform. The covariance between the coefficients and the state levels is expressed by the $(P+1) \times 2$ matrix

$$\begin{aligned}\boldsymbol{\Sigma}_{\hat{\theta}L} &= \operatorname{cov}(\hat{\boldsymbol{\theta}}, \boldsymbol{L}) \\ &= \operatorname{cov}(\boldsymbol{T}\boldsymbol{Y}, \boldsymbol{H}_L \boldsymbol{Y}) \\ &= \boldsymbol{T}\boldsymbol{\Sigma}_Y \boldsymbol{H}_L^T \\ &= \left(\boldsymbol{M}^T \boldsymbol{\Sigma}_r^{-1} \boldsymbol{M}\right)^{-1} \boldsymbol{M}^T \boldsymbol{\Sigma}_r^{-1} \boldsymbol{H}_r \boldsymbol{\Sigma}_Y \boldsymbol{H}_L^T.\end{aligned}$$

C. Transition Duration

Transition duration, i.e., the difference between two reference level instants, is a commonly reported quantity for steplike pulses. The correlation between the two instants and the top and bottom state levels must be considered to correctly propagate uncertainty from the covariance matrix of the waveform to the uncertainty in the transition duration.

The estimated transition duration Δt_{BA} from reference level A to reference level B is $\hat{t}_B - \hat{t}_A$, where $\hat{t}_B$ and $\hat{t}_A$ are obtained by use of the procedures described in the previous section. Specifically, the estimated polynomial coefficients are

$$\hat{\boldsymbol{\theta}}_A = \boldsymbol{T}_A \boldsymbol{Y}$$

for $\hat{t}_A$ and

$$\hat{\boldsymbol{\theta}}_B = \boldsymbol{T}_B \boldsymbol{Y}$$

for $\hat{t}_B$, where

$$\boldsymbol{T}_A = \left(\boldsymbol{M}_A^T \boldsymbol{\Sigma}_A^{-1} \boldsymbol{M}_A\right)^{-1} \boldsymbol{M}_A^T \boldsymbol{\Sigma}_A^{-1} \boldsymbol{H}_A$$

$$\boldsymbol{T}_B = \left(\boldsymbol{M}_B^T \boldsymbol{\Sigma}_B^{-1} \boldsymbol{M}_B\right)^{-1} \boldsymbol{M}_B^T \boldsymbol{\Sigma}_B^{-1} \boldsymbol{H}_B.$$

The squared standard uncertainty that is associated with Δt_{BA} is evaluated by propagation of uncertainty and is given by

$$u^2(\Delta t_{BA}) = \boldsymbol{J}_R \begin{pmatrix} \boldsymbol{\Sigma}_{\hat{\theta}_A} & \boldsymbol{\Sigma}_{\hat{\theta}_A \hat{\theta}_B} & \boldsymbol{\Sigma}_{\hat{\theta}_A L} \\ \boldsymbol{\Sigma}_{\hat{\theta}_A \hat{\theta}_B}^T & \boldsymbol{\Sigma}_{\hat{\theta}_B} & \boldsymbol{\Sigma}_{\hat{\theta}_B L} \\ \boldsymbol{\Sigma}_{\hat{\theta}_A L}^T & \boldsymbol{\Sigma}_{\hat{\theta}_B L}^T & \boldsymbol{\Sigma}_L \end{pmatrix} \boldsymbol{J}_R^T \tag{9}$$

where $\boldsymbol{J}_R$ is the Jacobian of $\hat{t}_B - \hat{t}_A$ with respect to $(\hat{\boldsymbol{\theta}}_A, \hat{\boldsymbol{\theta}}_B, \boldsymbol{L})$. The terms $\boldsymbol{\Sigma}_{\hat{\theta}_A}$, $\boldsymbol{\Sigma}_{\hat{\theta}_B}$, $\boldsymbol{\Sigma}_L$, $\boldsymbol{\Sigma}_{\hat{\theta}_A L}$, and $\boldsymbol{\Sigma}_{\hat{\theta}_B L}$ are found in the same way as described in the previous section. The new term $\boldsymbol{\Sigma}_{\hat{\theta}_A \hat{\theta}_B}$, describing the covariance between the two polynomial fits, is found as

$$\boldsymbol{\Sigma}_{\hat{\theta}_A \hat{\theta}_B} = \boldsymbol{T}_A \boldsymbol{\Sigma}_Y \boldsymbol{T}_B^T.$$

V. Additive and Multiplicative Errors

Let $y_j(t_i)$ denote the measurement of the jth two-state pulsed waveform at time t_i. A model for $y_j(t_i)$ that accounts for additive and multiplicative errors (with respect to the nominal waveform) is given by

$$y_j(t_i) = (1 + \alpha_j) S(t_i) + \beta_{ij} \tag{10}$$

where $S(\cdot)$ is the nominal pulsed waveform, and α_j and β_{ij} are normally distributed uncorrelated random variables with mean zero and variances a^2 and b^2, respectively. With this model, we have

$$\operatorname{var}[y(t_i)] = a^2 S^2(t_i) + b^2 \tag{11}$$

$$\operatorname{cov}[y(t_i), y(t_{i'})] = a^2 S(t_i) S(t_{i'}), \quad i \neq i'. \tag{12}$$

This simple model accounts for many of the error sources that we encounter in our laboratory, including the effect of uncertain knowledge about the gain in our oscilloscope, the temperature-dependent pulse amplitude variations in our pulse generators, and the Johnson noise of our samplers. The limiting case of $a = 0$ results in a measurement model with uncorrelated additive errors, and the case of $b = 0$ produces a model with correlated multiplicative errors. Different mixtures of additive and multiplicative errors can be chosen by varying a and b.

The simulation studies of Section VI show that the covariance matrix of (4) must be modified in cases where uncorrelated additive errors are the main source of errors. In those cases, (4) substantially underestimates the true variation of the estimated state levels. The reason is as follows. If $y_{(j)}$ in (2) were selected randomly, arithmetic mean L_1 would converge at the $h^{-1/2}$ rate. However, the data are selected from the shortest half, and L_1 converges at the $h^{-1/3}$ rate [15] as I_1 becomes large. Therefore, (4), which is obtained without including the variation of the shorth process, needs to be adjusted. One simple way to compensate for the different convergence rates is to multiply the uncertainty of L_1 that is obtained by the covariance-matrix approach by $h^{1/2}/h^{1/3} = h^{1/6}$.

We use a simple simulated example to illustrate the adjustment for a single level. We generate $I = 200$ samples from the waveform in (10) with $t_i = i/2048$, $S(t_i) = 1$, $i = 1, \ldots, I$, $a = 0$, and $b = 1$. The shortest interval that contains 50% of the 200 samples is determined, and the mean of the $(101 = 200/2 + 1)$ samples inside this shortest interval is computed. We denote this mean by L. We repeat this process 1000 times. The standard deviation of the 1000 means is found to be 0.200, which is an accurate estimate of the uncertainty of L. However, the uncertainty of L based on (4) is approximately equal to $b/\sqrt{101} = 0.099$. With the adjustment factor $101^{1/6} = 2.158$, we use $2.158 \times 0.099 = 0.21$ as the uncertainty of L. We also use other values of I and b in the simulation; the results seem to confirm the effectiveness of the adjustment.

Authorized licensed use limited to: IEEE Xplore. Downloaded on February 6, 2009 at 18:49 from IEEE Xplore. Restrictions apply.

In a more typical two-level waveform, the values of h and k that are used in (2) and (3) to calculate L_1 and L_2 may not be the same; therefore, the elements of the covariance matrix in (4) must be adjusted separately. We replace the covariance matrix in (4) with

$$\begin{pmatrix} u^2(L_1)h^{1/3} & u(L_1,L_2)(hk)^{1/6} \\ u(L_1,L_2)(hk)^{1/6} & u^2(L_2)k^{1/3} \end{pmatrix} \tag{13}$$

where $u(L_1, L_2)$ is the off-diagonal element, and $u^2(L_1)$ and $u^2(L_2)$ are the first and second diagonal elements of $\mathbf{\Sigma}_L$ in (4), respectively.

The adjustment is needed only under the uncorrelated additive error model. Under this model, the nominal covariance matrix of $\boldsymbol{Y}$ is a diagonal matrix with each diagonal element equal to b^2, and the nominal covariance matrix $\mathbf{\Sigma}_L$ is given by

$$\begin{pmatrix} b^2/h & 0 \\ 0 & b^2/k \end{pmatrix}.$$

That is, L_1 and L_2 are uncorrelated. Based on this result, we use a simple test to determine whether the adjustment should be applied, i.e., to test whether L_1 and L_2 are correlated. First, we calculate the correlation of L_1 and L_2 as

$$r = \frac{u(L_1, L_2)}{u(L_1)u(L_2)}.$$

Then, Fisher's z transformation [18] is employed to obtain

$$z = \frac{1}{2}\log\left(\frac{1+r}{1-r}\right).$$

Let $p = \min(h, k)$. If

$$\sqrt{p-3}|z| \leq 1.96 \tag{14}$$

we conclude that L_1 and L_2 are not correlated, and the covariance matrix in (13) should replace the covariance matrix in (4). Otherwise, the covariance matrix from (4) is used without modification.

In practice, a will not be exactly equal to zero; that is, L_1 and L_2 are correlated. However, the adjustment is still needed if the correlation is not *significantly* different from zero. The z-test is simply used for this purpose and should not be used to test if the measurement model is additive.

If one of the states in the waveform is zero, and $a \neq 0$, then the above z-test will be ineffective for determining whether the adjustment should be applied. A detailed discussion on how to adjust $\mathbf{\Sigma}_L$ under these conditions is given in Appendix C.

VI. Simulation Results

To verify (5) and (9) and the algorithms that we use to evaluate them, we use a standard steplike pulse $S(t_i)$ (shown in Fig. 1 and described in Appendix D) in (10) with different values of a and b to generate $y_j(t_i)$ and perform Monte Carlo simulations. For our first simulation, we set $a = 0$ and vary b between 0.01 and 0.05 with an increment of 0.01 [scaled relative to $S(t)$] to investigate how well the propagation of uncertainty approach estimates the variation of the pulse parameters. For each value of b, we generated $J = 1024$ waveforms $(j = 1, \ldots, J)$. For each waveform, we used $t_i = 5i/2048$, $i = 1, \ldots, 128$. This gives 33 points typically in each state after selecting the shortest half of the state, i.e., $h = k = 33$. The mean waveform $\bar{y}(t_i)$ and the (ii')th element of the 128×128 sample covariance matrix $\boldsymbol{S}$ based on the 1024 waveforms were calculated as

$$\bar{y}(t_i) = \frac{1}{J}\sum_{i=1}^{J} y_j(t_i)$$

$$S_{ii'} = \frac{1}{J-1}\sum_{j=1}^{J}\left(y_j(t_i) - \bar{y}(t_i)\right)\left(y_j(t_{i'}) - \bar{y}(t_{i'})\right)$$

where $i' = 1, \ldots, I$.

We first used the proposed shorth procedure on the mean waveform $\bar{y}(t_i)$ to determine the pulse states, the pulse amplitude A, and the transition duration Δt_{BA}. We then used the sample covariance matrix $\boldsymbol{S}$ as $\mathbf{\Sigma}_Y$ in propagating the uncertainty of A, denoted by u_A, using (4) and (5), and in propagating the uncertainty of Δt_{BA}, denoted by u_{td}, using (9). The modified $\mathbf{\Sigma}_L$ in (13) was used throughout. The simulation was repeated 20 times for each value of b. Figs. 2 and 3 display the results corresponding to the amplitude and the transition duration, respectively.

For each value of b, the scatter of the 20 u_A's is shown by the dots in each column of Fig. 2. It also shows, using the empty circles, the pooled standard deviation of the 20 A's, which is an adequate estimate of the uncertainty of the amplitude estimate.

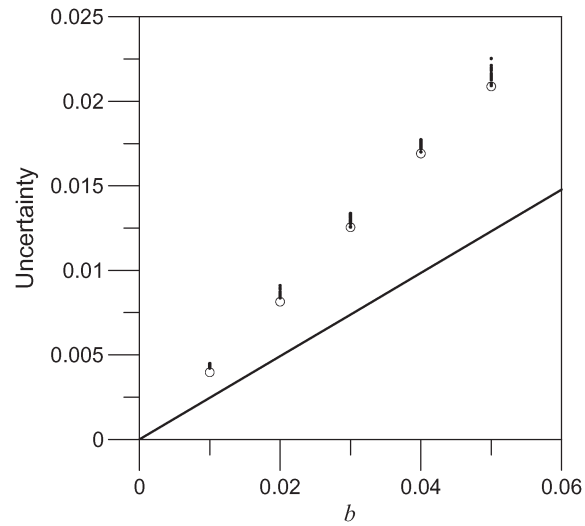

Fig. 2. Scatter of the 20 uncertainty estimates (by propagation of uncertainty) associated with amplitude estimates for each value of b with $a = 0$ (dots). The empty circles show the pooled standard deviation of the 20 amplitude estimates. The line shows the values of $\sqrt{2/33}b$, which are the uncertainty estimates using the unadjusted covariance matrix $\mathbf{\Sigma}_L$.

Authorized licensed use limited to: IEEE Xplore. Downloaded on February 6, 2009 at 18:49 from IEEE Xplore. Restrictions apply.

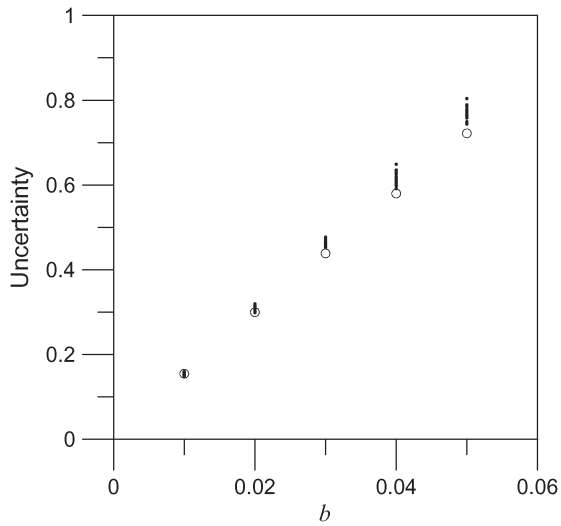

Fig. 3. Scatter of the 20 uncertainty estimates (by propagation of uncertainty) associated with transition duration estimates for each value of b with $a = 0$ (dots).The empty circles show the pooled standard deviation of the 20 transition duration estimates.

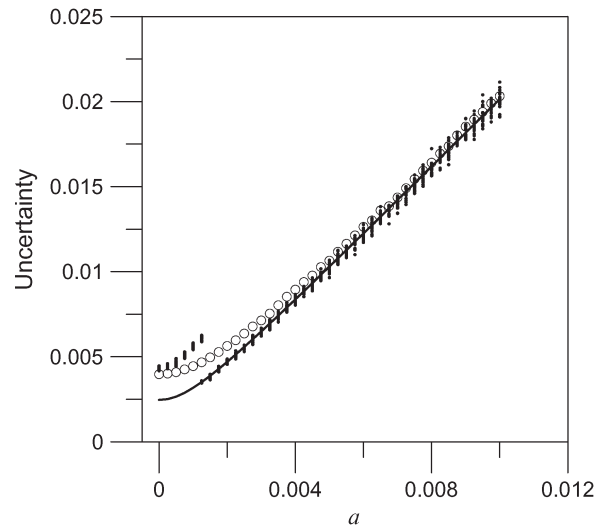

Fig. 4. Scatter of the 20 uncertainty estimates (by propagation of uncertainty) associated with amplitude estimates for each value of a with $b = 0.01$ (dots). The empty circles show the pooled standard deviation of the 20 amplitude estimates. The line shows the values of $\sqrt{0.0002/33 + 3.959a^2}$, which are the uncertainty estimates using the unadjusted covariance matrix $\mathbf{\Sigma}_L$.

The "best" squared uncertainty estimate for the amplitude using the unmodified $\mathbf{\Sigma}_L$ is given by

$$\begin{pmatrix} -1 & 1 \end{pmatrix} \begin{pmatrix} b^2/33 & 0 \\ 0 & b^2/33 \end{pmatrix} \begin{pmatrix} -1 \\ 1 \end{pmatrix} = \frac{2}{33} b^2.$$

It is the "best" because b is assumed known and not estimated. Values of $\sqrt{2/33}b$ are shown by the line in Fig. 2. It clearly indicates that they greatly underestimate the uncertainty of the amplitude.

Similarly, Fig. 3 shows the scatter of the 20 u_{td}'s (dots) and the pooled standard deviation of the 20 Δt_{BA}'s (the empty circles). Figs. 2 and 3 show that the uncertainty that is calculated by the use of the proposed propagation of uncertainty technique closely tracks the actual standard deviation of the pulse parameters, with bias slowly increasing for large errors.

In our next simulation, we set $b = 0.01$ and vary a from 0 to 0.01 [scaled relative to $S(t)$] with an increment of 0.00025 to investigate our ability to accurately estimate the pulse parameter uncertainty in the presence of multiplicative errors. We simulated the waveforms and calculated the pulse parameter standard deviation (based on the 20 simulations), and also propagated the uncertainty as before. However, this time, we performed the test for significant correlation in $\mathbf{\Sigma}_L$ using (14) and modified $\mathbf{\Sigma}_L$ using (13) when appropriate. The results are shown in Figs. 4 and 5 with the same designation for dots and empty circles as those in Figs. 2 and 3.

Fig. 4 shows that at $a = 0.00125$ (the sixth value of a), the dots scatter on both sides of the circle, indicating that the uncertainty estimates can either overestimate or underestimate the variation of the pulse amplitude. This is because, at this point, there are approximately equal contributions from additive and multiplicative errors in the measurements, resulting in an approximately equal probability of passing or failing the z-test of (14). The bias is positive if the z-test is passed, and the modified $\mathbf{\Sigma}_L$ is used; the bias is negative if the z-test is failed,

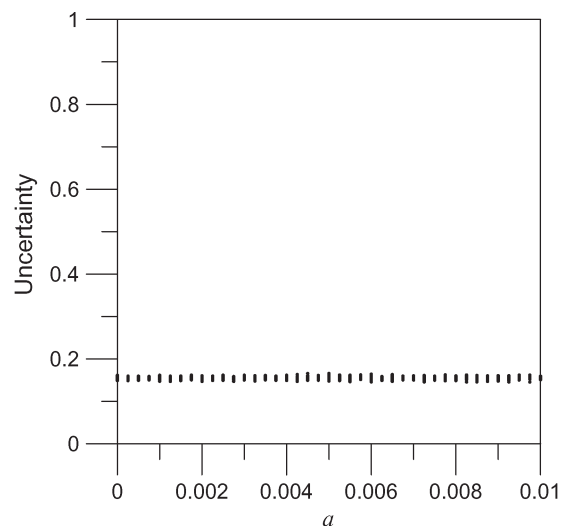

Fig. 5. Scatter of the 20 uncertainty estimates (by propagation of uncertainty) associated with the estimates of transition duration for each value of a with $b = 0.01$ (dots). Note that the vertical scale is the same as that used in Fig. 3 to emphasize the observation that the transition duration is invariant with respect to the multiplicative error standard deviation a.

and $\mathbf{\Sigma}_L$ is used without modification. The magnitude of the bias when $a = 0.00125$ is about 30% and is acceptably low for our applications in either case.

The "best" uncertainty estimate for the amplitude when only the unmodified $\mathbf{\Sigma}_L$ is used, i.e., without performing the test for significant correlation in $\mathbf{\Sigma}_L$, is given by

$$\sqrt{\frac{b^2}{h} + \frac{b^2}{k} + 3.959a^2} = \sqrt{\frac{2}{33}0.01^2 + 3.959a^2}. \qquad (15)$$

This is obtained as follows. The covariance matrix of $\boldsymbol{Y}$ is obtained using (11) and (12) with the appropriate approximate

Authorized licensed use limited to: IEEE Xplore. Downloaded on February 6, 2009 at 18:49 from IEEE Xplore. Restrictions apply.

values of $S(t_i)$ (either -1 or 0.9897). Based on this covariance matrix, the covariance matrix $\mathbf{\Sigma}_L$ is obtained using (4) as

$$\begin{pmatrix} b^2/h + a^2 & -0.9897a^2 \\ -0.9897a^2 & b^2/k + 0.9897^2 a^2 \end{pmatrix}.$$

The result then follows.

The values of (15) are shown by the line in Fig. 4. The "dot" and the "line" agree within the scatter of the data except when a is small. When a is small, the probability of passing the test in (14) is high, resulting in the use of the modified $\mathbf{\Sigma}_L$ for calculating the uncertainty estimates. We need to point out that the "line" was calculated assuming a known value of a.

Fig. 5 shows, as expected, that the uncertainty of the transition duration is independent of the multiplicative error. We used the same Y-axis scale as in Fig. 3 for ease of comparison.

VII. Discussion

It is important to remember that the quantity that has physical meaning in any waveform measurement is the measurand, be it voltage, current, optical power, or other physical quantity that is being measured as a function of time. Pulse parameters are defined by the algorithm that is used to transform the waveform measurements to a metric of (typically) one dimension. It is reasonable to expect that different algorithms will return slightly different pulse parameters for a given waveform. Algorithms should be designed to have specific desired properties, such as the following informal (and probably incomplete) list. The algorithm should

1) return the intuitively expected value in certain well-behaved situations;
2) be robust against small perturbations of the waveform, such as the additive error or small time shifts [19] (provided that the pulse has sufficiently settled at the endpoints);
3) use an (approximately) linear measurement equation for the measurand, so that the uncertainty of the parameter estimate can be calculated using the covariance-matrix approach that is used in this paper;
4) have a minimal number of arbitrary parameters.

In this paper, we have described algorithms that are capable of sorting the waveform data into an arbitrary number of states and determining the state levels without the use of histograms. These algorithms meet the above criteria. We have focused on the shorth for locating state levels, although a matrix operator for the mean can be constructed that could also be used with the covariance approach for propagating uncertainty. The mean is biased by clustered points in the transition region, but has the advantage that its variance converges as $h^{-1/2}$. On the other hand, the shorth is robust against such outliers, whereas its variance converges at a slower rate of $h^{-1/3}$. We have used the matrix operators, along with the waveform covariance matrix, to propagate uncertainties in the estimated state levels and the pulse parameters. By demonstrating agreement with the Monte Carlo simulations, we demonstrated that our transformations are sufficiently linear as to make our approach valid.

The covariance approach is an extremely powerful technique, which has application extending beyond the conventional pulse parameters in [1] provided that the transformations and the error sources are sufficiently linear. Although we have used a simple two-state waveform and the 1-D pulse parameters of the state level, the reference level instant, and the transition duration as examples, these methods can be generalized to more complicated waveforms, frequency-domain metrics [4], and vector metrics, such as the vector $\boldsymbol{L}$ described in this paper or a vector consisting of two or more reference level instants. These two vectors could be used, for example, to characterize eye opening in a digital system.

Appendix A
Calculating Covariance Matrices

Type A uncertainty analysis evaluates uncertainty using the statistical analysis of the measurand itself. Consider a set $\{\boldsymbol{y}_j; j = 1, \ldots, J\}$ of waveform vectors, each of length I, obtained from J repeated measurements. Each waveform can be considered an I-dimensional random variable. Type A analysis is used to quantify random variations in the measured waveform in terms of the sample covariance matrix $\boldsymbol{S}$, as was done in Section VI.

The determination of the confidence regions that are associated with $\boldsymbol{S}$ is beyond the scope of this paper. However, as a rule of thumb, the number of measurements should be much greater than the dimensionality of the ultimate pulse parameter that is being extracted. A somewhat more detailed discussion of confidence regions can be found in [4, Sec. VII].

Type B uncertainty analysis is used to quantify uncertainty using other methods. For example, a waveform might be a function $\boldsymbol{f}$ of some scaler quantity p, where p might be the temperature of the waveform generator or the bias on a particular component in the generator. In this case, we might generate the Jacobian in (1) using a finite-difference method, as described in [4]. That is, we measure the waveform under identical conditions with the exception of changing p by a small amount δ, obtaining waveforms $\boldsymbol{f}(p)$ and $\boldsymbol{f}(p+\delta)$. The Jacobian describing the sensitivity of the waveform generator to variations in p is then an $I \times 1$ vector, i.e.,

$$\boldsymbol{J}_p = \frac{\boldsymbol{f}(p+\delta) - \boldsymbol{f}(p)}{\delta}.$$

If the variance of p is σ_p^2, then the $I \times I$ covariance matrix $\mathbf{\Sigma}_p$ expressing the uncertainty in the generated waveform due to variations in p is found as

$$\mathbf{\Sigma}_p = \boldsymbol{J}_p \left[\sigma_p^2\right] \boldsymbol{J}_p^T.$$

Notice that Type A analysis could also be used to characterize the uncertainty due to p if the repeated measurements were taken while randomly varying p and keeping all other factors effectively constant.

Authorized licensed use limited to: IEEE Xplore. Downloaded on February 6, 2009 at 18:49 from IEEE Xplore. Restrictions apply.

APPENDIX B
JACOBIAN FOR QUADRATIC FIT

For example, if $P = 2$, the root of the equation

$$\hat{\theta}_2 \hat{t}_r^2 + \hat{\theta}_1 \hat{t}_r + \hat{\theta}_0 - L_1 - f(L_2 - L_1) = 0$$

is given by

$$\hat{t}_r = R(\hat{\boldsymbol{\theta}}, \boldsymbol{L}) = \frac{-\hat{\theta}_1 \pm \sqrt{\hat{\theta}_1^2 - 4\hat{\theta}_2 \left[\hat{\theta}_0 - L_1 - f(L_2 - L_1)\right]}}{2\hat{\theta}_2}$$

with the sign chosen to satisfy the constraint $t_{q+1} \le \hat{t}_r \le t_{q+N}$. Then, the Jacobian matrix $\boldsymbol{J}_R$ in (8) is given by

$$\begin{aligned}\boldsymbol{J}_R &= \left(\frac{\partial R}{\partial \hat{\theta}_0}, \frac{\partial R}{\partial \hat{\theta}_1}, \frac{\partial R}{\partial \hat{\theta}_2}, \frac{\partial R}{\partial L_1}, \frac{\partial R}{\partial L_2}\right) \\ &= \left(\mp\frac{1}{Q}, \frac{\pm\hat{\theta}_1 - Q}{2\hat{\theta}_2 Q}, \frac{\hat{\theta}_1 \mp Q}{2\hat{\theta}_2} \mp \frac{\hat{\theta}_0 - y_r}{\hat{\theta}_2 Q}, \pm\frac{1-f}{Q}, \pm\frac{f}{Q}\right)\end{aligned}$$

where

$$Q = \sqrt{\hat{\theta}_1^2 - 4\hat{\theta}_2(\hat{\theta}_0 - y_r)}$$

and $y_r = L_1 + f(L_2 - L_1)$.

APPENDIX C
CASE WHERE ONE STATE IS ZERO

Suppose that the two states are zero and one. Using the results in (11) and (12), it is shown that the nominal covariance matrix of the states is given by

$$\begin{pmatrix} b^2/h & 0 \\ 0 & b^2/k + a^2 \end{pmatrix}.$$

Consequently, the test in (14) is likely to pass, indicating the need to adjust both uncertainties. In this particular case, it is necessary to adjust only the uncertainty corresponding to the state whose level is zero. Therefore, if one of the states is zero, instead of performing the z-test, one should examine the covariance matrix of the states. If the uncertainty corresponding to the nonzero state is relatively large compared to the uncertainty corresponding to the zero state (implying $a \neq 0$), then only the uncertainty corresponding to the zero state should be adjusted.

If $h \approx k$, we can use the statistic [18]

$$F = \frac{u^2(L_2)}{u^2(L_1)}$$

to test for the significance of a. Specifically, if $F > F_{0.95,k-1,h-1}$, we conclude that a is significantly greater than zero, where F_{α,n_1,n_2} is the α quantile of an F distribution with n_1 and n_2 degrees of freedom.

APPENDIX D
STANDARD STEP FUNCTION THAT IS USED FOR MONTE CARLO SIMULATION

For the Monte Carlo simulations, we define the sample times $t_i = 5i/2048$, with $i = 1, \ldots, 128$, and generate the following offset step function:

$$S(t_i) = \mathrm{Re}\left\{cH(t_i - \tau_s)\left[\sum_n \frac{a_n}{\nu_n}\left[e^{-2\pi i \nu_n (t_i - \tau_s)} - 1\right]\right]\right\} - d$$

where $c = 2$, $d = 1$, $\tau_s = 0.140625$, and the step function $H(\cdot)$ is 0 for arguments that are less than zero and 1 for arguments that are greater than zero. The following values of ν_n and a_n make $S(t)$ a fourth-order Chebyshev filter response with cutoff frequency equal to 1:

ν_1	$0.92461260260237 - 0.24315230680940\,i$
ν_2	$0.38298707993899 - 0.58702159682156\,i$
ν_3	$-0.38298707993899 - 0.58702159682156\,i$
ν_4	$-0.92461260260237 - 0.24315230680940\,i$
a_1	$0.18945349227976 - 0.20419547447615\,i$
a_2	$-0.64072041135120 + 0.20419547447615\,i$
a_3	$0.64072041135120 + 0.20419547447615\,i$
a_4	$-0.18945349227976 - 0.20419547447615\,i$

We multiply the above values of ν_n and a_n by the cutoff frequency $f_c = 34.0600$ to achieve nominal 10%–90% transition duration of 12.0058 and state levels $L_1 = -1.0000$ and $L_2 = 0.9897$, although the pulse level asymptotically approaches 0.990074380 with increasing time.

ACKNOWLEDGMENT

The authors would like to thank A. Dienstfrey for many useful discussions, for providing the coefficients in Appendix D, and for his careful review of the manuscript. They would also like to thank G. Stenbakken for his careful review of the manuscript. They are also grateful to S. Narayan, who patiently worked on Monte Carlo simulations of pulse parameter measurements using the histogram technique during the summer of 2006. Although this paper is not about the histogram approach, his work helped the authors develop a "philosophy" of pulse parameter measurements that they hope they have conveyed in this paper.

REFERENCES

[1] *IEEE Standard on Transitions, Pulses, and Related Waveforms*, Institute of Electrical and Electronics Engineers, IEEE Std. 181-2003, Jul. 2003.
[2] N. G. Paulter and D. R. Larson, "Pulse parameter uncertainty analysis," *Metrologia*, vol. 39, no. 2, pp. 143–155, 2002.
[3] N. G. Paulter and D. R. Larson, "The effect of tilt on waveform state levels and pulse parameters," in *Proc. IMTC*, Como, Italy, May 18–20, 2004, pp. 1296–1300.
[4] D. F. Williams, A. Lewandowski, T. S. Clement, C. M. Wang, P. D. Hale, J. M. Morgan, D. A. Keenan, and A. Dienstfrey, "Covariance-based uncertainty analysis of the NIST electrooptic sampling system," *IEEE Trans. Microw. Theory Tech.*, vol. 54, no. 1, pp. 481–491, Jan. 2006.
[5] F. A. Graybill, *Theory and Application of the Linear Model*. North Scituate, MA: Duxbury, 1976.

Authorized licensed use limited to: IEEE Xplore. Downloaded on February 6, 2009 at 18:49 from IEEE Xplore. Restrictions apply.

[6] N. M. Ridler and M. J. Salter, "An approach to the treatment of uncertainty in complex S-parameter measurements," *Metrologia*, vol. 39, no. 3, pp. 295–302, 2002.
[7] R. Willink and B. D. Hall, "A classical method for uncertainty analysis with multidimensional data," *Metrologia*, vol. 39, no. 4, pp. 361–369, 2002.
[8] B. D. Hall, "On the propagation of uncertainty in complex-valued quantities," *Metrologia*, vol. 41, no. 3, pp. 173–177, Jun. 2004.
[9] B. D. Hall, "Some considerations related to the evaluation of measurement uncertainty for complex-valued quantities in radio frequency measurements," *Metrologia*, vol. 44, no. 6, pp. L62–L67, Dec. 2007.
[10] M. Cox, M. Dainton, P. Harris, and N. Ridler, "The evaluation of uncertainties in the analysis of calibration data," in *Proc. Instrum. Meas. Technol. Conf.*, May 24–26, 1999, pp. 1093–1098.
[11] P. D. Hale, D. F. Williams, A. Dienstfrey, C. M. Wang, A. Lewandowski, T. S. Clement, and D. A. Keenan, "Complete waveform characterization at NIST," in *Proc. Conf. Precision Electromagn. Meas.*, Jun. 8–13, 2008, pp. 680–681.
[12] D. F. Williams, P. D. Hale, and T. S. Clement, "Calibrated 200 GHz waveform measurement," *IEEE Trans. Microw. Theory Tech.*, vol. 53, no. 4, pp. 1384–1389, Apr. 2005.
[13] J. A. Hartigan, *Clustering Algorithms*. Hoboken, NJ: Wiley, 1975.
[14] O. M. Solomon, D. R. Larson, and N. G. Paulter, "Comparison of some algorithms to estimate the low and high state level of pulses," in *Proc. IEEE Instrum. Meas. Conf.*, Budapest, Hungary, May 21–23, 2001, pp. 96–100.
[15] P. Rousseeuw and A. Leroy, *Robust Regression and Outlier Detection*. Hoboken, NJ: Wiley, 2003.
[16] F. R. Hampel, E. M. Ronchetti, P. J. Rousseeuw, and W. A. Stahel, *Robust Statistics*. Hoboken, NJ: Wiley, 1986.
[17] N. R. Draper and H. Smith, *Applied Regression Analysis*. Hoboken, NJ: Wiley, 1981.
[18] G. W. Snedecor and W. G. Cochran, *Statistical Methods*. Ames, IA: Iowa State Univ. Press, 1980.
[19] D. R. Larson, N. G. Paulter, and D. I. Bergman, "Pulse parameter dependence on transition occurrence instant and waveform epoch," *IEEE Trans. Instrum. Meas.*, vol. 54, no. 4, pp. 1520–1526, Aug. 2005.

Paul D. Hale (M'01–SM'01) received the Ph.D. degree in applied physics from the Colorado School of Mines, Golden, in 1989.

Since 1989, he has been with the Optoelectronics Division, National Institute of Standards and Technology (NIST), Boulder, CO, where he conducts research on broadband optoelectronic devices and signal metrology. His current technical work focuses on extending both time- and frequency-domain optoelectronic measurements to beyond 110 GHz, implementing novel covariance-based uncertainty analysis that can be used for time- and frequency-domain quantities, and disseminating NIST traceability through high-speed electronic and optoelectronic measurement services. Since 1996, he has been the Leader of the High-Speed Measurements Project in the Sources and Detectors Group. He has authored over 50 technical publications.

Dr. Hale was the recipient of the Department of Commerce Bronze, Silver, and Gold Awards, of two Automatic Radio Frequency Techniques Group Best Paper Awards, and of the NIST Electrical Engineering Laboratory's Outstanding Paper Award. From June 2001 to March 2007, he was an Associate Editor of optoelectronics/integrated optics for the IEEE JOURNAL OF LIGHTWAVE TECHNOLOGY.

C. M. Jack Wang received the Ph.D. degree in statistics from the Colorado State University, Fort Collins, in 1978.

Since 1988, he has been with the Statistical Engineering Division, National Institute of Standards and Technology, Boulder, CO. He has authored over 70 journal articles. His research interests include statistical metrology and the application of statistical methods to physical sciences.

Dr. Wang was the recipient of the Department of Commerce Bronze Medals and of several awards from the American Statistical Association (ASA). He is a Fellow of the ASA.

Authorized licensed use limited to: IEEE Xplore. Downloaded on February 6, 2009 at 18:49 from IEEE Xplore. Restrictions apply.